Tokyo Climate Center, Japan Meteorological Agency

TCC News

No. 22 Autumn 2010

Contents

El Niño Outlook (October 2010 – April 2011)

La Niña conditions are present in the equatorial Pacific, and are likely to persist into boreal winter.

Pacific Ocean

In September 2010, the SST deviation from a sliding 30-year mean SST averaged over the NINO.3 region (5°N – 5°S, 150°W – 90°W) was -1.3°C. The five-month running-mean value of NINO.3 SST deviations was -0.8°C for July, and the Southern Oscillation Index for September was +2.3. In September, negative SST anomalies prevailed over most of the equatorial Pacific except near Indonesia, where positive values were recorded (Figures 1 (b) and 3 (a)). Subsurface temperature anomalies were positive in the western equatorial Pacific, and were remarkably negative in its central and eastern parts (Figures 2 (b) and 3 (b)). In the equatorial Pacific, convective activity near the date line was calmer than normal. Easterly wind anomalies in the lower troposphere prevailed in the western and central equatorial Pacific. These oceanic and atmospheric conditions are consistent with those seen during La Niña events.

In the equatorial Pacific, persistent easterly anomalies in the lower troposphere brought continued negative subsurface temperature anomalies in its central and eastern parts. These negative anomalies will in turn cause SSTs to remain below normal.

According to JMA's El Niño prediction model, NINO.3 SST deviations will continue to be below normal into boreal winter (Figure 4).

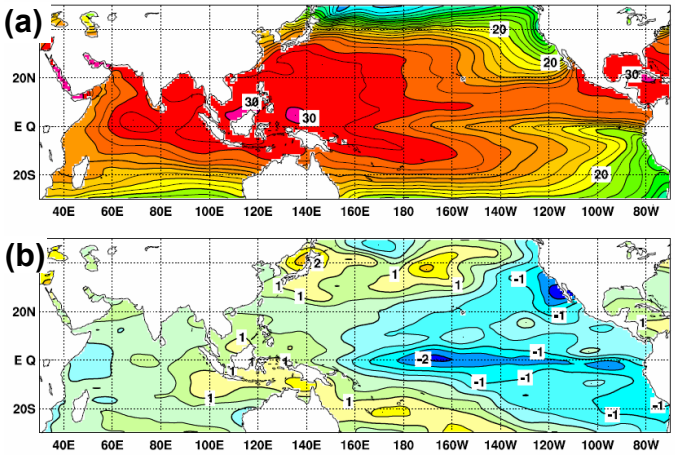

Figure 1 Monthly mean (a) sea surface temperatures (SSTs) and (b) SST anomalies in the Indian and Pacific Ocean areas for September 2010
Contour intervals are 1°C in (a) and 0.5°C in (b). The base period for the normal is 1971 – 2000.

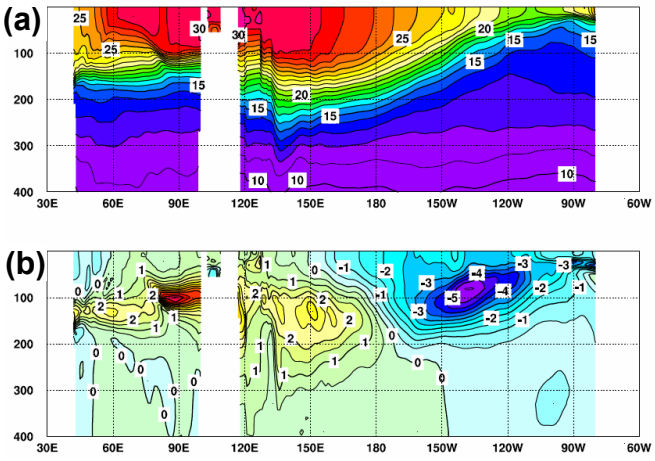

Figure 2 Monthly mean depth-longitude cross sections of (a) temperatures and (b) temperature anomalies in the equatorial Indian and Pacific Ocean areas for September 2010
Contour intervals are 1°C in (a) and 0.5°C in (b). The base period for the normal is 1979 – 2004.

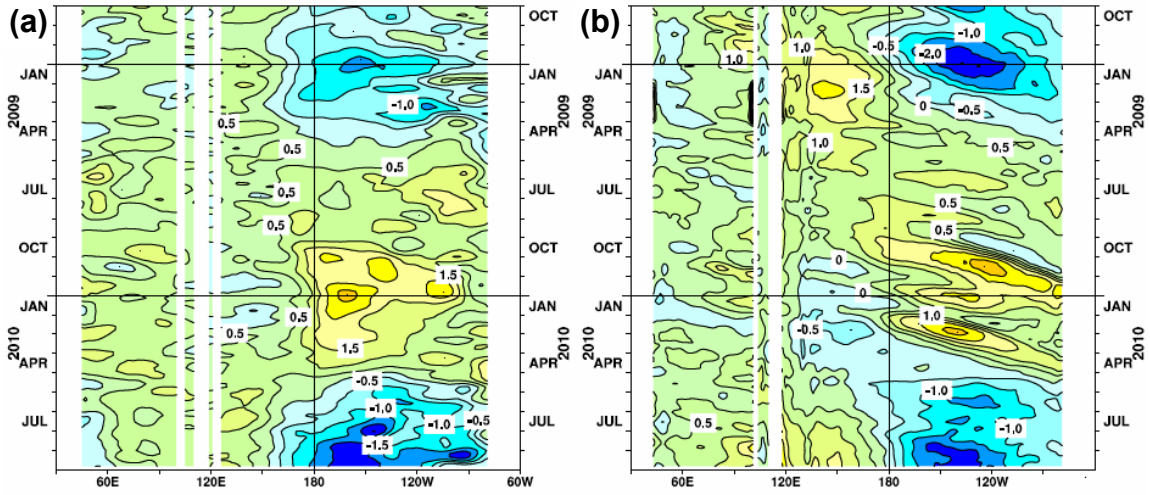

Figure 3 Time-longitude cross sections of (a) SST and (b) ocean heat content (OHC) anomalies along the equator in the Indian and Pacific Ocean areas
OHCs are defined here as vertical averaged temperatures in the top 300 m. The base periods for the normal are 1971 – 2000 for (a) and 1979 – 2004 for (b).

Considering all the above observations and model result, it can be concluded that La Niña conditions are present in the equatorial Pacific and are likely to persist into boreal winter.

It is likely that the SST averaged over the NINO.WEST region (Eq. – 15°N, 130°E – 150°E) will continue to be near or above normal into boreal winter.

Indian Ocean

The SST averaged over the tropical Indian Ocean (IOBW) region (20°S – 20°N, 40°E – 100°E) has been near normal since August. It is likely to gradually become below normal in the months ahead.

Impact on the global climate

In September, conditions were much warmer than normal in East Asia and over the islands to the east of Australia. This was consistent with common climate patterns seen in past La Niña events.

(Ichiro Ishikawa, Climate Prediction Division)

* The SST normals for the NINO.WEST region (Eq. – 15° N, 130°E – 150°E) and the IOBW region (20°S – 20°N, 40° E – 100°E) are defined as linear extrapolations with respect to a sliding 30-year period, in order to remove the effects of long-term trends.

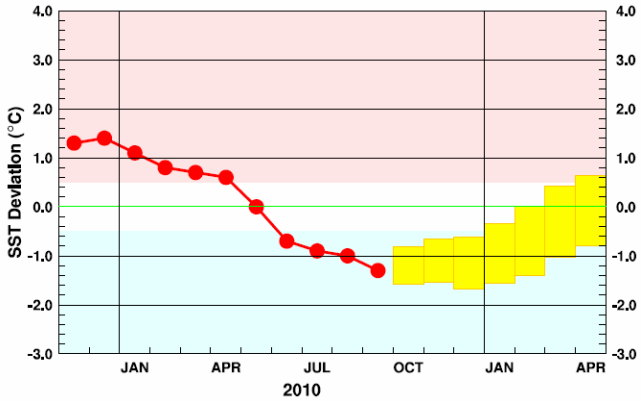

Figure 4 Outlook of NINO.3 SST deviation produced by the El Niño prediction model
This figure shows a time series of monthly NINO.3 SST deviations. The thick line with closed circles shows observed SST deviations, and the boxes show the values produced for the next six months by the El Niño prediction model. Each box denotes the range into which the SST deviation is expected to fall with a probability of 70%.

JMA's Seasonal Numerical Ensemble Prediction for Winter 2010/2011

According to JMA's seasonal ensemble prediction system, a negative anomaly in the central and eastern equatorial Pacific is expected to continue in winter 2010/2011, indicating that the current La Niña event is likely to persist during this period. Corresponding to sea surface temperature (SST) conditions, the JMA system indicates active rainfall around the Maritime Continent, the South Pacific Convergence Zone (SPCZ) and the eastern tropical Indian Ocean, and suppressed rainfall in the central part of the tropical Pacific. Below-normal surface temperatures are expected around the eastern part of China and over Southeast Asia, while above-normal temperatures are expected in northern Japan.

1. Introduction

This article outlines JMA's dynamical seasonal ensemble prediction for winter 2010/2011 (December 2010 – February 2011, referred to as DJF), which was used as a basis for the Agency's operational cold-season outlook issued on 25 October, 2010. The prediction shown here is based on the seasonal ensemble prediction system with the Atmosphere-Ocean General Circulation Model (AOGCM). Please refer to the column for details of this system.

Section 2 presents predicted global SST anomalies, and Section 3 describes predicted circulation fields in the tropics and sub-tropics associated with these anomalies. Finally, the predicted circulation fields in the mid- and high latitudes of the Northern Hemisphere are explained in Section 4.

2. SST anomalies (Figure 5)

In September 2010, remarkably negative and positive SST anomalies were seen in the central to eastern equatorial Pacific and western tropical Pacific, respectively. These conditions indicate that the current La Niña event, which appeared in the summer of 2010, is well developed. According to JMA's El Niño outlook, the La Niña event is expected to continue into winter (see also JMA's El Niño Outlook in this issue).

The predicted SST anomalies are shown in Figure 5. Below-normal SSTs are predicted in central to eastern parts of the equatorial Pacific, while above-normal SSTs are predicted in the western tropical Pacific and the tropical Atlantic.

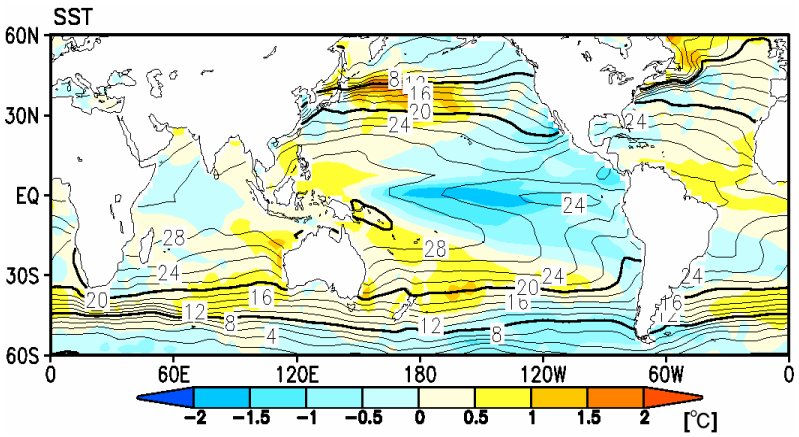

Figure 5 Predicted SST (contours) and SST anomalies (shading) for December 2010 – February 2011 (ensemble mean of 51 members)

3. Prediction in the tropics and sub-tropics (Figure 6)

Predicted precipitation shows conditions typical of those seen during La Niña events. Below-normal precipitation is predicted in the central equatorial Pacific, while above-normal precipitation is predicted over the eastern Indian Ocean, the Maritime Continent and the South Pacific Convergence Zone (SPCZ).

In the upper troposphere, a negative velocity potential anomaly at 200 hPa (i.e., more divergent) is predicted over the Maritime Continent, reflecting active precipitation in the region, while positive (i.e., more convergent) anomalies are predicted from the central part of the tropical Pacific and the western part of the Indian Ocean. The predicted stream function at 200 hPa shows an anti-cyclonic anomaly over Southeast Asia and a cyclonic anomaly in the northeast tropical Pacific associated with the precipitation anomalies. In the lower troposphere, a cyclonic anomaly is predicted over the northeastern part of the Indian Ocean, while an anti-cyclonic anomaly is expected in the northwestern part of the tropical Pacific. These features are consistent with those seen during La Niña events.

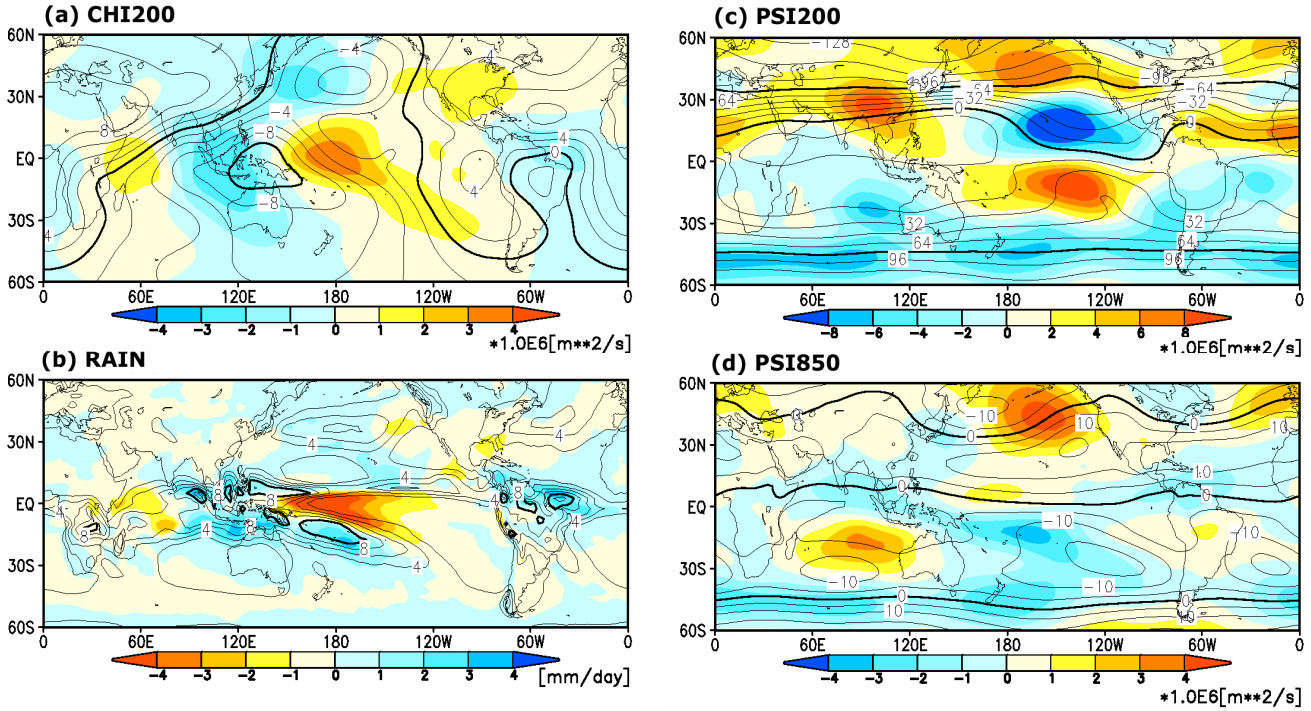

Figure 6 Predicted atmospheric fields from 60°N – 60°S for December 2010 – February 2011 (ensemble mean of 51 members)

(a) Velocity potential at 200 hPa (contours) and anomaly (shading). The contour interval is 2 x 10^6 m^2/s.
(b) Precipitation (contours) and anomaly (shading). The contour interval is 2 mm/day.
(c) Stream function at 200 hPa (contours) and anomaly (shading). The contour interval is 16 x 10^6 m^2/s.
(d) Stream function at 850 hPa (contours) and anomaly (shading). The contour interval is 5 x 10^6 m^2/s.

4. Prediction in the mid- and high latitudes of the Northern Hemisphere (Figures 7 and 8)

The seasonal ensemble system predicts positive 500-hPa geopotential height anomalies over the North Pacific and negative anomalies from the eastern and southern part of Japan to the western part of Northeast Asia. Below-normal surface temperatures are expected around East and Southeast Asia, while above-normal temperatures are expected in northern Japan.

(Yuhei Takaya, Climate Prediction Division)

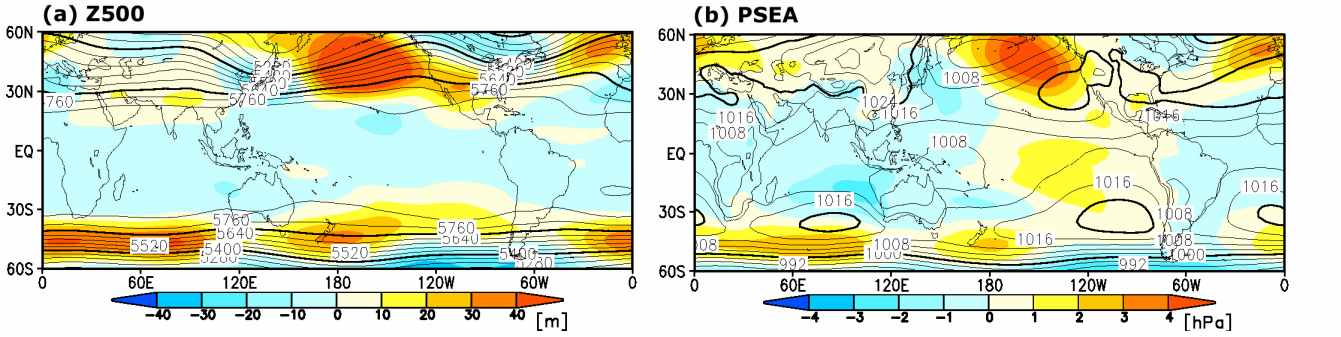

Figure 7 Predicted atmospheric fields from 60°N – 60°S for December 2010 – February 2011 (ensemble mean of 51 members)
(a) 500 hPa height (contours) and anomaly (shading). The contour interval is 60 m.
(b) Sea level pressure (contours) and anomaly (shading). The contour interval is 4 hPa.

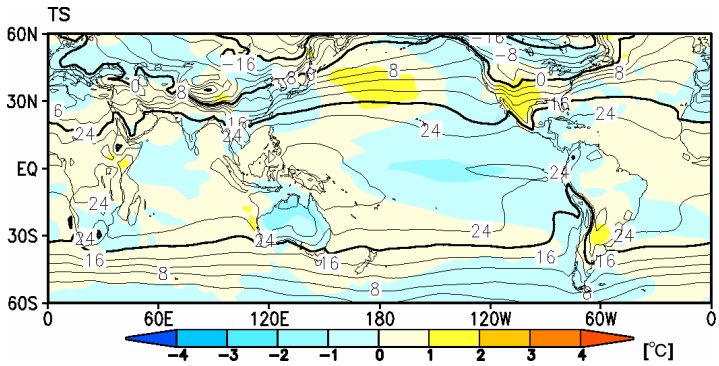

Figures 8 Predicted surface (2-m) temperatures for December 2010 – February 2011 (ensemble mean of 51 members)
The contour interval is 2 degrees. The shading indicates 2-m temperature anomaly.

JMA's Seasonal Ensemble Prediction System

JMA operates a seasonal Ensemble Prediction System (EPS) using the Atmosphere-Ocean General Circulation Model (AOGCM) to make seasonal predictions beyond a one-month time range. The EPS produces perturbed initial conditions by means of a combination of the initial perturbation method and the lagged average forecasting (LAF) method. The prediction consists of 51 members from the latest six initial dates (9 members are run every five days). Details of the prediction system and verification maps based on 30-year hindcast experiments (1979 – 2008) are available at http://ds.data.jma.go.jp/tcc/tcc/products/model/.

Cold-season Outlook for Winter 2010/2011 in Japan

JMA's seasonal forecast for winter 2010/2011, issued on 22 September 2010, indicates no significant temperature anomalies for any part of Japan.

1. Oceanic conditions

In August 2010, the SST deviation from a sliding 30-year mean SST averaged over the NINO.3 region was -1.0° C. The five-month running-mean value of NINO.3 SST deviations was -0.4°C for June, and the Southern Oscillation Index for August was +1.9. In August, remarkably positive SST anomalies were seen in the western equatorial Pacific, and remarkably negative anomalies were found from the area west of the date line to eastern parts. Subsurface temperature anomalies were positive in the western equatorial Pacific, and were remarkably negative in its central and eastern parts. In the equatorial Pacific, convective

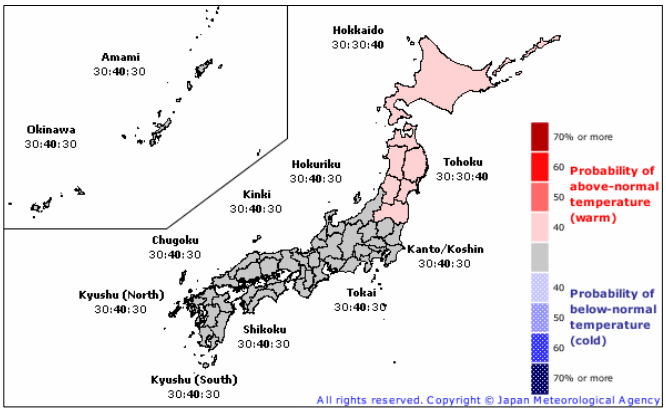

Figure 9 Outlook for winter 2010/2011 temperature probability in Japan

activity near the date line was calmer than normal. Easterly wind anomalies in the lower troposphere prevailed in the western and central equatorial Pacific. These oceanic and atmospheric conditions are consistent with those seen during La Niña events. In the equatorial Pacific, persistent easterly anomalies in the lower troposphere brought continued negative subsurface temperature anomalies in its central and eastern parts. These negative anomalies will in turn cause SSTs to remain below normal. According to JMA's couple-model, NINO.3 SST deviations will continue to be below normal into boreal winter (December-January-February).

Considering all the above observations, it can be concluded that La Niña conditions are present in the equatorial Pacific and are likely to persist into boreal winter. It is likely that the SST averaged over the NINO.WEST region will continue to be near or above normal from boreal autumn to winter.

2. Numerical prediction

The SST anomaly pattern predicted by the JMA couple-model is very similar to that seen during La Niña events (i.e., above normal in the western Pacific and below normal in the central and eastern Pacific).

In association with this pattern, the ensemble averaged atmospheric circulation anomaly pattern predicted by the model is also very similar to that seen during La Niña events in the tropics and the sub-tropics as outlined below.

In the lower tropospheric (850 hPa) stream function field, cyclonic circulation anomaly is clearly predicted from southern India to the South China Sea. In the upper tropospheric (200 hPa) stream function field, anti-cyclonic circulation anomaly is clearly predicted from northern India to southern China, and cyclonic circulation anomaly is predicted around Japan. Corresponding to the circulation anomalies over East Asia, the subtropical jet streams will shift northward over China and southward over Japan, suggesting a strong winter monsoon around the latter. This meandering of the subtropical jet streams is expected as a result of the predicted La Niña-type SST anomalies.

In the mid- and high latitudes, a slightly positive phase of the Arctic Oscillation (AO) is predicted by the JMA couple-model. The positive (negative) phase of the AO tends to cause a weak (strong) winter monsoon and above-normal (below-normal) temperatures in northern Japan. However, the spread among each ensemble member is large, and the hindcast (30 years from 1979 to 2008) suggests that the model does not have a level of skill sufficient to predict the AO.

3. Long-term trends and decadal variation

Long-term upward trends are clearly seen in winter mean temperatures over Japan except in its northern part, where the winter mean temperature shows large year-to-year fluctuations and recent ten-winter mean temperatures have been near normal (although slightly warmer). Winter precipitation has tended to be above normal on the Pacific side of northern, eastern and western Japan since the end of the 1990s.

The tropospheric thickness temperature averaged over the mid-latitudes of the Northern Hemisphere (30°N – 50° N), which is positively correlated with temperatures in Japan, has tended to be above normal since 2006. According to the JMA couple-model, it will remain above normal into boreal winter (December-January-February).

4. Conclusion

According to numerical prediction, below-normal temperatures are expected for Japan in winter (except in its northern part) in response to La Niña conditions. However, considering the long-term trend, the temperature is in fact likely to be higher than the results of numerical prediction suggest. In northern Japan, both numerical prediction and the long-term trend suggest the likelihood that temperatures will be slightly higher than normal in winter.

5. Outlook summary

Predicted cold-season mean temperatures and total precipitation amounts show no significant anomalies for any part of Japan. Cold-season snowfall amounts on the Sea of Japan side of the country are expected to be near or below normal with a 40% probability for each in northern Japan (Figures 9, 10 and 11).

(Hajime Takayama, Climate Prediction Division)

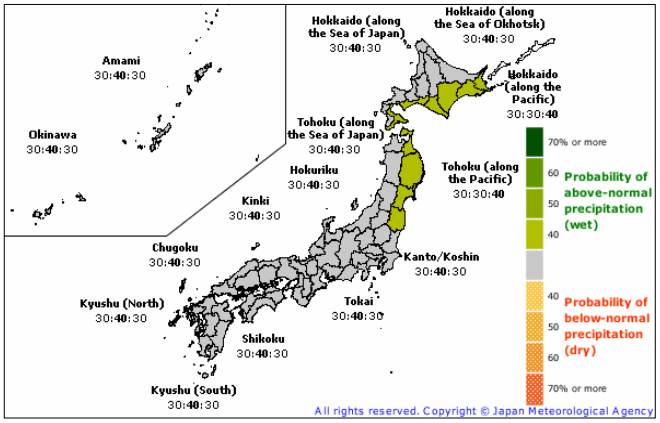

Figure 10 Outlook for winter 2010/2011 precipitation probability in Japan

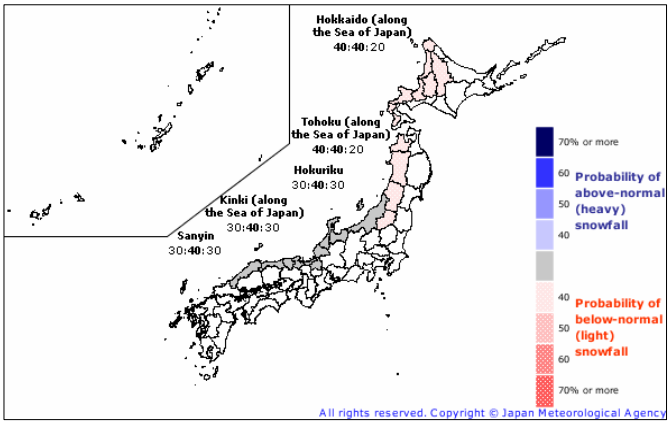

Figure 11 Outlook for winter 2010/2011 snowfall probability in Japan

1. Monsoon activity and atmospheric circulation

Convective activity (inferred from the seasonal mean (i.e., that from June to September) of outgoing longwave radiation (OLR)) associated with the Asian summer monsoon was enhanced across a broad area including the Maritime Continent, the Arabian Sea, Pakistan, the South China Sea and the area to the north of the Philippines (Figure 12). In the period from June to the first half of July, however, it was suppressed from northern India to the Indochina Peninsula and to the east of the Philippines. Across the western and central equatorial Pacific, suppressed convection was seen from June 2010.

In the lower troposphere, monsoon westerlies were stronger than normal over the Arabian Sea, and were weaker than normal in the Bay of Bengal and over the South China Sea (Figure 13 (b)). The monsoon trough around the Philippines was weaker than normal. Anticyclonic circulation anomalies were prominent over a wide area from the North Pacific and East Asia to northern India. In the upper troposphere, the Tibetan High was extended northeastward and westward from its normal position (Figure 13 (a)). In the equatorial region, easterly wind anomalies were predominant over the Indian Ocean, while westerly anomalies were seen over the western and central Pacific.

The active phase of the Madden-Julian Oscillation (MJO) propagated eastward with a period of approximately 30 days (Figure 14). The area of active convection originally enhanced by the MJO to the south of India was seen to propagate northward around India (Figure 15).

(Shotaro Tanaka, Climate Prediction Division)

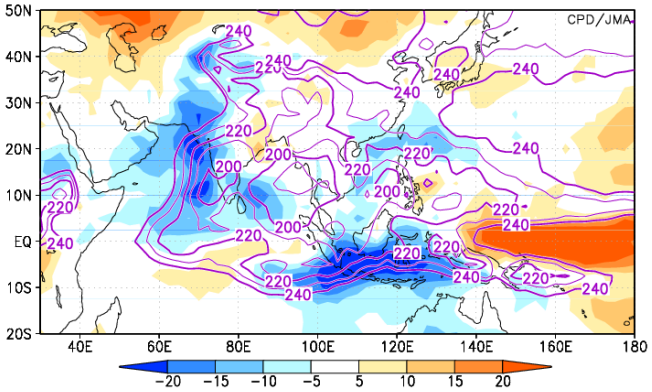

Figure 12 Four-month mean outgoing longwave radiation (OLR) and its anomaly for June – September 2010
The contours indicate OLR (W/m^2) at intervals of 10 W/m^2, and the color shading denotes OLR anomalies from the 1979 – 2004 average.

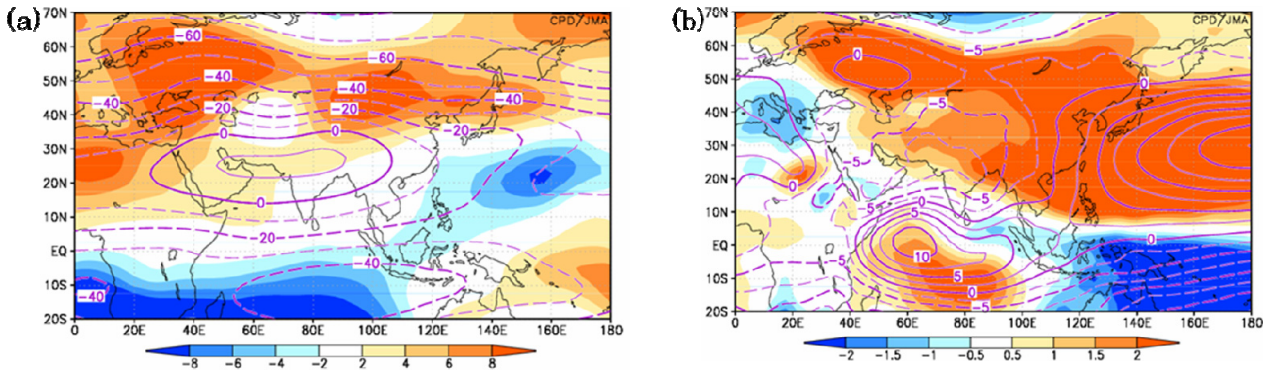

Figure 13 Four-month mean stream function and its anomaly for June – September 2010
(a) The contours indicate 200-hPa stream function (m^2/s) at intervals of 10 × 10^6 m^2/s, and the color shading indicates 200-hPa stream function anomalies from the 1979 – 2004 average. (b) The contours indicate 850-hPa stream function (m^2/s) at intervals of 2.5 × 10^6 m^2/s, and the color shading indicates 850-hPa stream function anomalies from the 1979 – 2004 average.

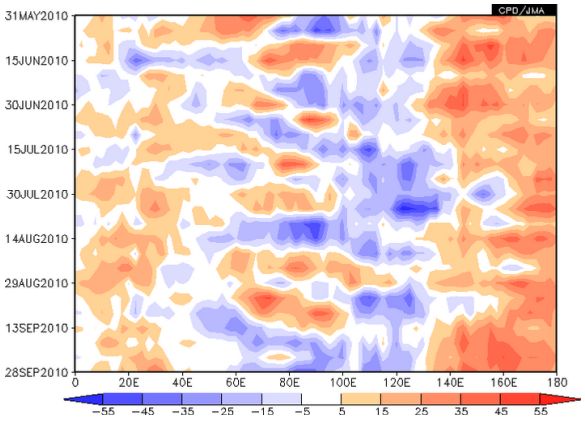

Figure 14 Time-longitude cross section of five-day mean OLR anomaly from June to September 2010 (5ºS – 5ºN mean)
The shading denotes OLR anomalies (W/m^2) from the 1979 – 2004 average. Cold and warm shading indicates above-normal and below-normal convective activity, respectively.

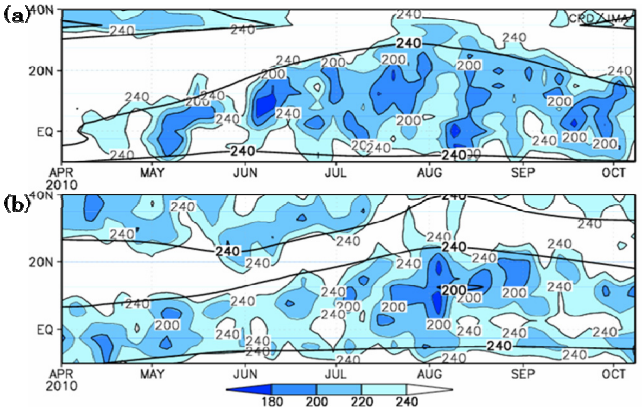

Figure 15 Latitude-time cross section of five-day mean OLR from April to September 2010 ((a) India (65 – 85ºE mean), (b) area east of the Philippines (125 – 145ºE mean))
The thick black lines indicate the climatological mean OLR for the period from 1979 to 2004. The shading denotes the OLR in 2010 (W/m^2).

2. Precipitation and temperature

Four-month total precipitation amounts based on CLIMAT reports during the monsoon season (June – September) were above 200% of the normal around Pakistan and in southern Indonesia, and were below 60% of the normal around Mongolia (Figure 16). They were mostly consistent with the distribution of OLR anomalies (Figure 12).

Four-month mean temperatures for the same period were higher than normal over most of eastern to southern Asia except around northern Pakistan and mid-southern China (Figure 17).

Extremely heavy precipitation was observed around Pakistan throughout the season. In contrast, extremely light precipitation was observed from the southern part of eastern Siberia to northern China in June and around Mongolia in July (figures not shown).

Monthly mean temperatures were extremely high in many regions throughout the period. The seasonal mean temperature in Japan for summer (i.e., the three-month period from June to August) was the highest since JMA's records began in 1898.

It was reported that heavy rains in Pakistan from 28 July to 7 August triggered floods in several parts of the country, resulting in 1,961 fatalities. It was also reported that a mudslide caused 1,765 fatalities in central China (Zhouqu County in Gansu Province) on 7 – 8 August.

3. Tropical cyclones

During the monsoon season, 11 tropical cyclones (TCs) of tropical storm (TS) intensity or higher formed over the western North Pacific (Figure 16 and Table 1). The number of formations was much lower than the 1971 – 2000 average of 16.4. A total of 7 among these 11 passed around the South China Sea and approached or hit southern China or Vietnam. Two TCs hit the main islands of Japan.

In July, Typhoon Conson caused 196 fatalities in the Philippines. In September, Typhoon Kompasu caused 12 fatalities in the Republic of Korea and 20 in the Democratic People's Republic of Korea.

Note: Disaster details are based on information from the UN's EM-DAT disaster database.

(Takafumi Umeda, Climate Prediction Division)

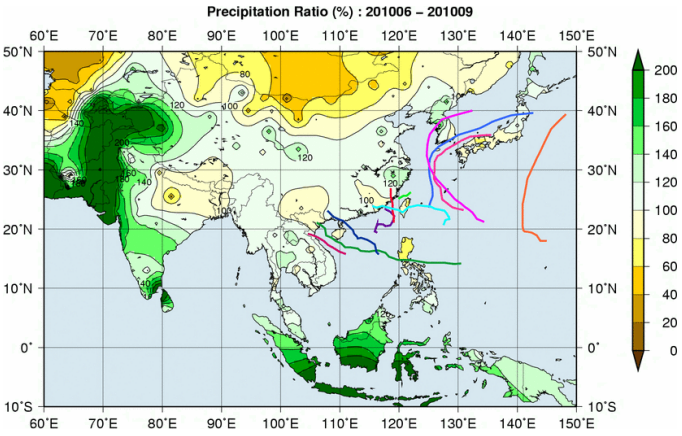

Figure 16 Four-month precipitation ratio (%) and tropical cyclone tracks in the northwestern Pacific from June to September 2010

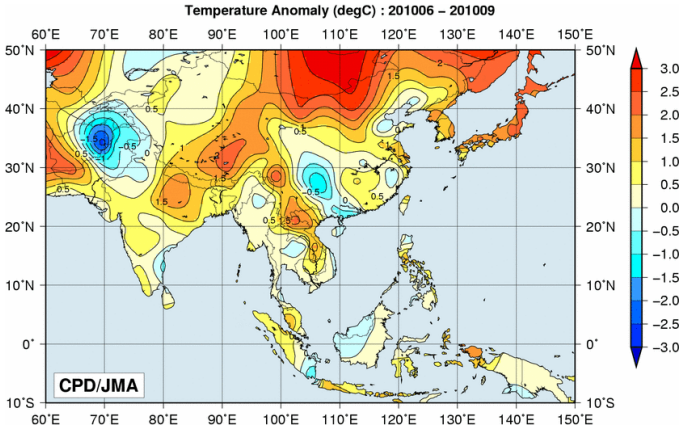

Figure 17 Four-month mean temperature anomaly (°C) from June to September 2010

Table 1 Tropical cyclones forming over the western North Pacific from June to September 2010

ID number	Name	Date (UTC)	Category[1)]	Maximum Winds[2)] (Knots)
T1002	Conson	7/12 – 7/17	TY	70
T1003	Chanthu	7/19 – 7/23	TY	70
T1004	Dianmu	8/8 – 8/12	STS	50
T1005	Mindulle	8/23 – 8/24	TS	45
T1006	Lionrock	8/28 – 9/2	STS	50
T1007	Kompasu	8/29 – 9/2	TY	80
T1008	Namtheun	8/30 – 8/31	TS	35
T1009	Malou	9/4 – 9/8	STS	50
T1010	Meranti	9/9 – 9/10	TS	45
T1011	Fanapi	9/15 – 9/20	TY	95
T1012	Malakas	9/21 – 9/25	TY	75

Note: Prepared by the RSMC Typhoon Center (provisional data for T1010 – T1012)
1) Intensity classification for tropical cyclones
TS: Tropical Storm
STS: Severe Tropical Storm
TY: Typhoon
2) Estimated maximum 10-minute mean wind

Status of the Antarctic Ozone Hole in 2010

The Antarctic ozone hole in 2010 covered its third-smallest area since 1990.

The Antarctic ozone hole has appeared for the last 30 years from late winter to early spring (August – December), peaking in September or early October. It is defined as the area where the total ozone column is equal to or less than 220 m atm-cm.

According to JMA's analysis of Aura OMI data, the ozone hole in 2010 appeared in August and expanded to reach a maximum area of 21.9 million km^2 on 25 September. This was 1.6 times as large as the Antarctic Continent (Figure 18), and represented its third-smallest area since 1990 after 1990 and 2002. The five spherical images in Figure 18 indicate total ozone column distributions in the Southern Hemisphere with the ozone hole shown in gray.

The Antarctic ozone hole is expected to return to pre-1980 levels in the late 21st century according to *WMO/UNEP Scientific Assessment of Ozone Depletion: 2010*. Continued close observation of the ozone layer is necessary to allow assessment of the hole's shrinkage.

(Seiji Miyauchi, Ozone Layer Monitoring Office, Atmospheric Environment Division)

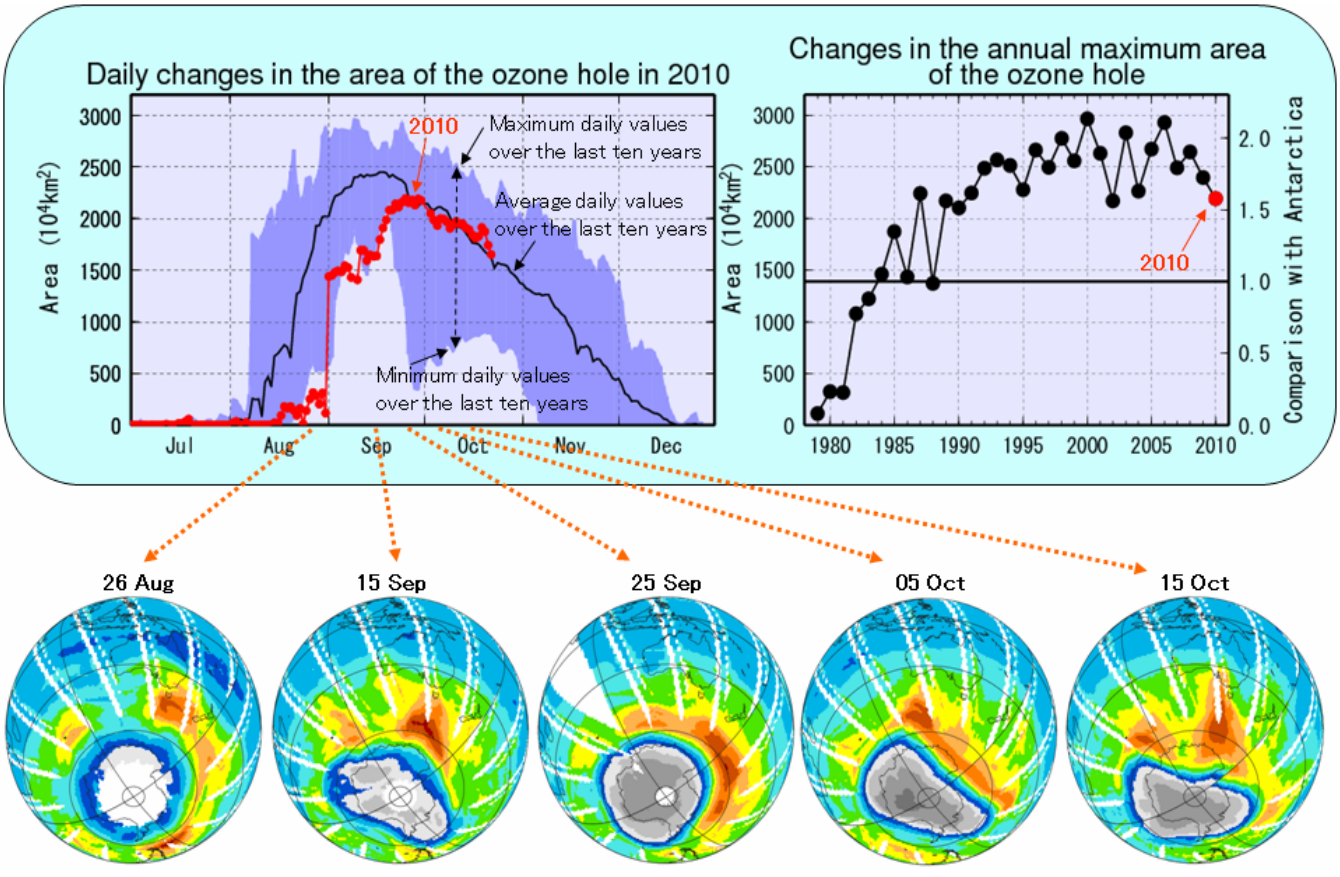

Figure 18 Daily changes in the area of the Antarctic ozone hole in 2010 (upper left), changes in its annual maximum area since 1979 (upper right), and total ozone distributions in the Southern Hemisphere on the indicated dates (bottom)
The Antarctic ozone hole is shown in gray in the spherical images at the bottom. These figures were made from Aura OMI data produced by KNMI (the Royal Netherlands Meteorological Institute) and processed using the ozone retrieval algorithm of NASA (the National Aeronautics and Space Administration).

Primary Factors Contributing to Japan's Extremely Hot Summer of 2010

In summer (June – August) 2010, Japan experienced nationwide record-breaking high temperatures. Shortly after this period on 3 September, JMA organized an extraordinary meeting of the Advisory Panel on Extreme Climate Events[1] to identify the characteristic atmospheric circulations causing these extremely hot conditions and to investigate the factors contributing to them. This report summarizes the atmospheric features and possible influences identified by the Advisory Panel as main background factors to Japan's hottest summer on record.

[1] The Advisory Panel, consisting of prominent experts on climate science from universities and research institutes, was established in June 2007 by JMA to investigate extreme climate events based on the latest knowledge and findings.

1. Temperature for summer 2010 in Japan

The seasonal mean temperature in Japan for summer 2010 (i.e., the three-month period from June to August) ousted that of summer 1994 from the top spot as the highest since JMA's records began in 1898, with a deviation[2] of +1.64°C from the 1971 – 2000 average (Figure 19). The temperature anomalies for the individual months were the fifth highest on record at +1.24°C for June, the eleventh highest at +1.42° C for July, and the highest at +2.25°C for August. In most regions of Japan, above-normal temperatures persisted during the summer.

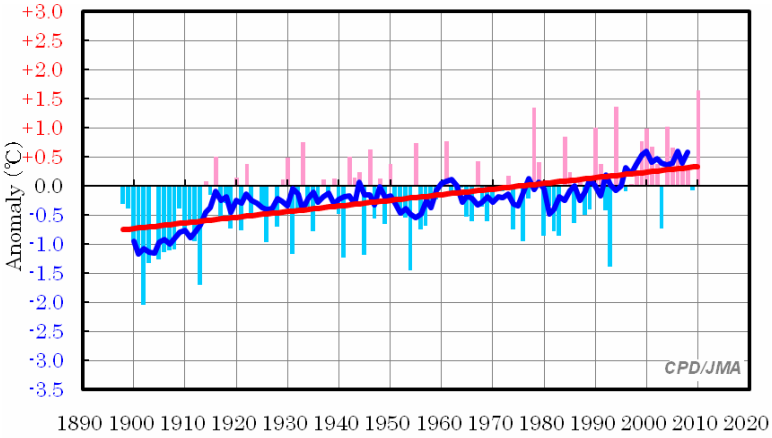

Figure 19 Long-term change in seasonal temperature anomalies for summer (June – August) in Japan
Anomalies are calculated as the average of temperature deviations from the 1971 – 2000 normal at the 17 observation stations[2]. The bars indicate anomalies of temperature for each summer. The blue line indicates the five-year running mean, and the red line shows the long-term linear trend.

2. Oceanographic conditions and convective activity in the tropics

In summer (June – August) 2010, a La Niña event followed the El Niño period that started in summer 2009 and ended in spring (March – May) 2010 (Figure 20). Sea surface temperatures (SSTs) were above normal in the Indian Ocean and the tropical Atlantic. This 2010 pattern echoed those of the La Niña events seen in 1988 and 1998 that rapidly occurred in spring and summer, respectively, after the end of an El Niño period in the previous season (Figure 21).

Convective activity (inferred from outgoing longwave radiation (OLR)) associated with the Asian summer monsoon was suppressed across a broad area from northern India to the Indochina Peninsula and to the east of the Philippines in the first half of summer 2010, and was enhanced in the Arabian Sea and from the Indochina Peninsula to the north of the Philippines in the second half (Figure 22). In the eastern Indian Ocean and on the Maritime Continent, convective activity was enhanced throughout the summer.

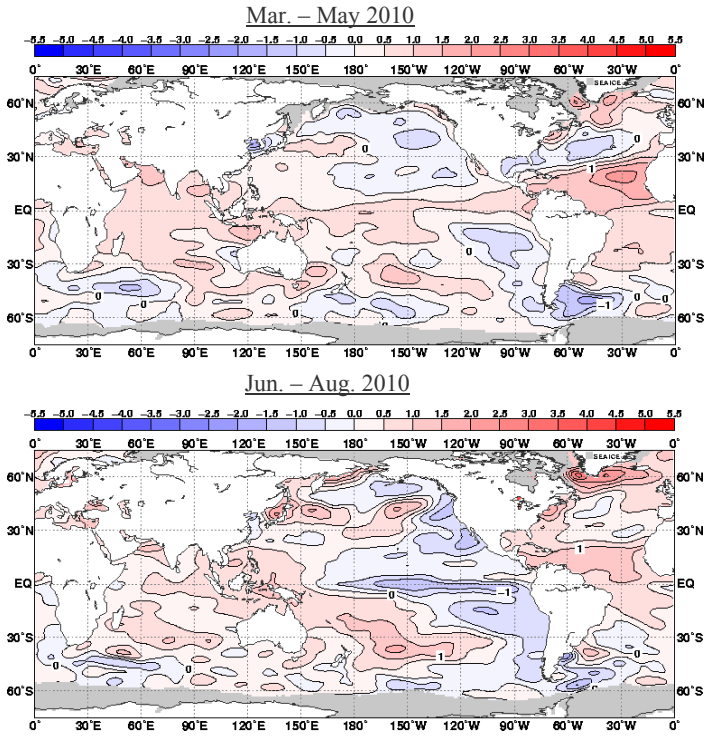

Figure 20 Three-month mean sea surface temperature anomalies for March – May (upper) and June – August (lower) 2010
The normal is the 1971 – 2000 average. The analysis data are COBE-SST.

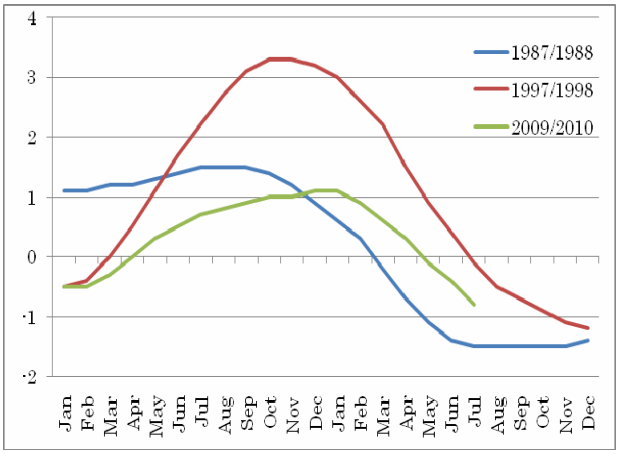

Figure 21 Time series of five-month running mean sea surface temperature deviations from the climatological mean based on a sliding 30-year period for NINO.3 (5°S – 5°N, 150°W – 90°W)

[2] Observatory stations representing the average temperature of Japan are selected from those deemed to be least influenced by the urban heat island phenomenon.

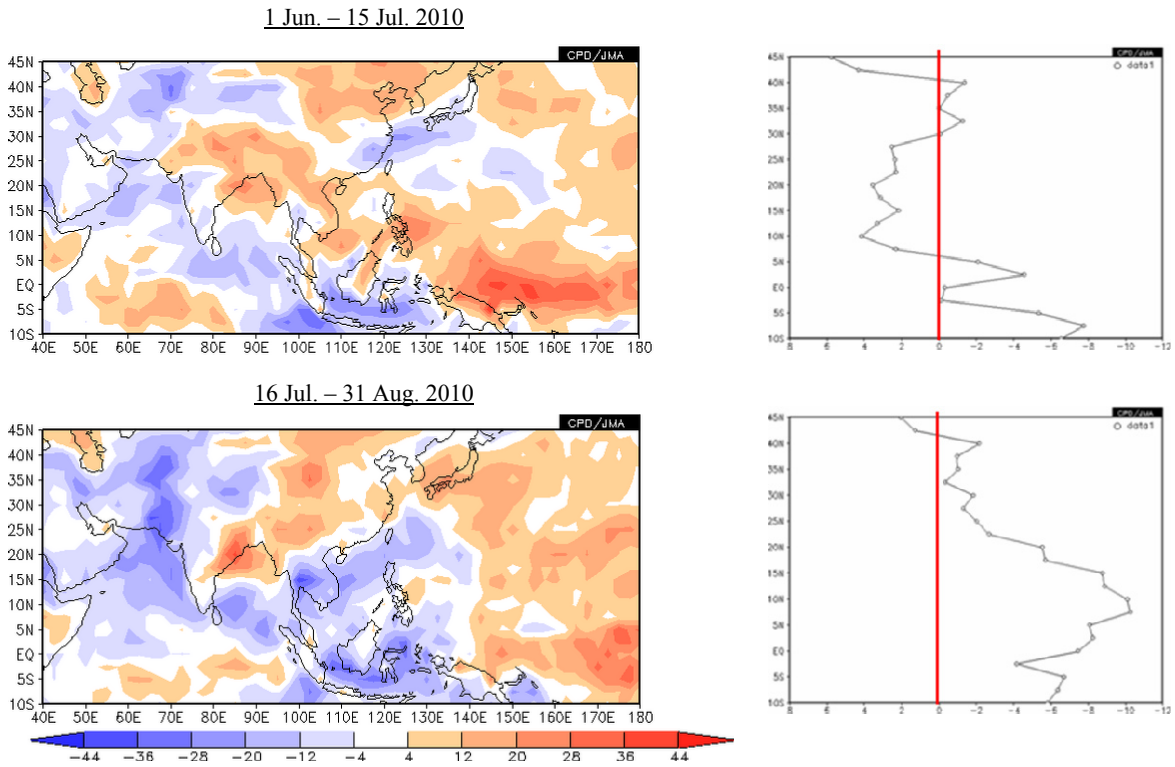

Figure 22 Outgoing Longwave Radiation (OLR) anomalies (unit: W/m^2)
Panels on the left: Cold and warm shading indicates enhanced and suppressed convective activity, respectively, in comparison with the normal (i.e., the 1979 – 2004 average). Panels on the right: Values indicate zonally averaged (60˚E – 140˚E) OLR anomalies in the corresponding panels on the left. Data provided by NOAA.

3. Characteristic atmospheric circulation causing Japan's hot summer and related factors

(1) Tropospheric air temperature

The zonally averaged tropospheric air temperature in the mid-latitudes of the Northern Hemisphere was the highest in summer (June – August) since 1979 (Figure 23). As shown in Figure 24, the values for 1998 and 1988 were the second and fourth highest, respectively, since 1979. Zonally averaged tropospheric thickness in the tropics reached an above-normal level in July 2009 and matured in the first half of 2010 (left panel of Figure 24). In June 2010, the thickness in the tropics remained above normal but decreased, while that in the mid-latitudes of the Northern Hemisphere rapidly increased and remained significantly above normal throughout the summer. Similar thickness anomaly evolution was identified in 1988 and 1998 (central and right panels of Figure 24).

As research so far (e.g., Angell, 1990) has indicated, tropospheric air temperatures increase on a global scale after El Niño events and then remain higher than normal for several months. Examination of past La Niña events shows a tendency for higher-than-normal tropospheric air temperatures in the mid-latitudes of the Northern Hemisphere, while those in the tropics have been below normal during summers with a La Niña event. This is consistent with the results of previous research (e.g., Seager et al., 2003).

It is therefore possible that zonally averaged tropospheric air temperatures in the mid-latitudes of the Northern Hemisphere were extremely high in summer 2010 from the influence of the El Niño event and partly due to the effects of the La Niña event.

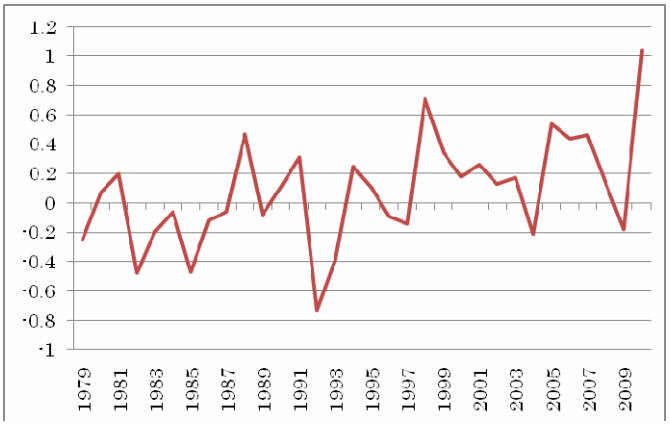

Figure 23 Time series of three-month (June – August) zonally averaged temperature anomalies (unit: K) in the mid-latitudes (30˚N – 60˚N) of the Northern Hemisphere calculated from thickness (850 – 300 hPa)
The base period for the normal is 1979 – 2004. The analysis data are JRA-25/JCDAS.

A warming trend can be identified in the zonally averaged tropospheric air temperature in the mid-latitudes of the Northern Hemisphere (Figure 23). This trend may be associated with global warming due to the buildup of anthropogenic greenhouse gases.

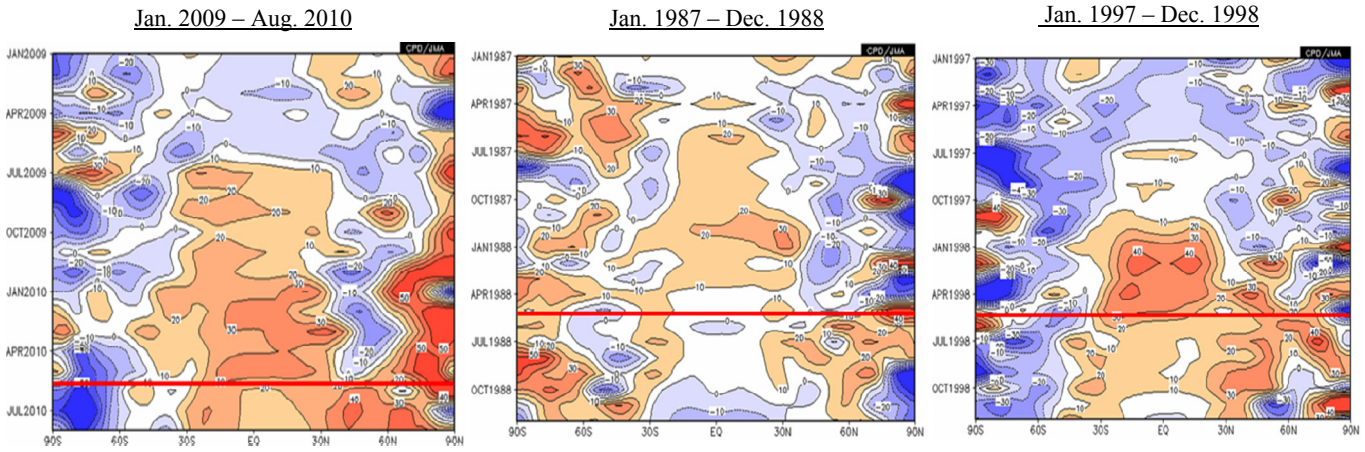

Figure 24 Time-latitude cross section of monthly, zonally averaged thickness anomaly (unit: m)
The base period for the normal is 1979 – 2004. The analysis data are JRA-25/JCDAS.

(2) Remarkably strong anticyclone over Japan

The subtropical jet stream in the vicinity of Japan showed a southward-shifted tendency from its normal position in the first half of summer 2010, while the jet stream shifted northward from its normal position with a frequent northward meander (a ridge of high pressure) in the second half (Figure 25). Corresponding to the features of the subtropical jet stream, the extension of the Tibetan High to Japan was weaker than normal in the first half of summer 2010, while it was stronger than normal and equivalent-barotropic highs developed and persisted over Japan in the second half (Figures 26 and 27).

As detailed in Section 2, convective activity was broadly enhanced in and around the Indian Ocean in the second half of summer 2010 (Figure 22). Considering that research so far (e.g., Krishnan and Sugi, 2001; Enomoto, 2004) indicates a link between the Asian summer monsoon and Japan's climate, statistical analysis was implemented to examine the relationship between convective activity linked to

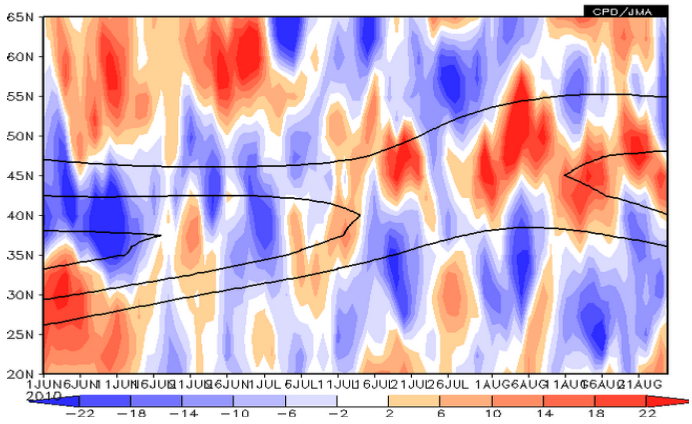

Figure 25 Latitude-time cross section of normals (black lines) and anomalies (colored shading) of the 200-hPa zonal wind speed averaged in the vicinity of Japan (125˚E – 145˚E)
The base period for the normal is 1979 – 2004. The analysis data are JRA-25/JCDAS.

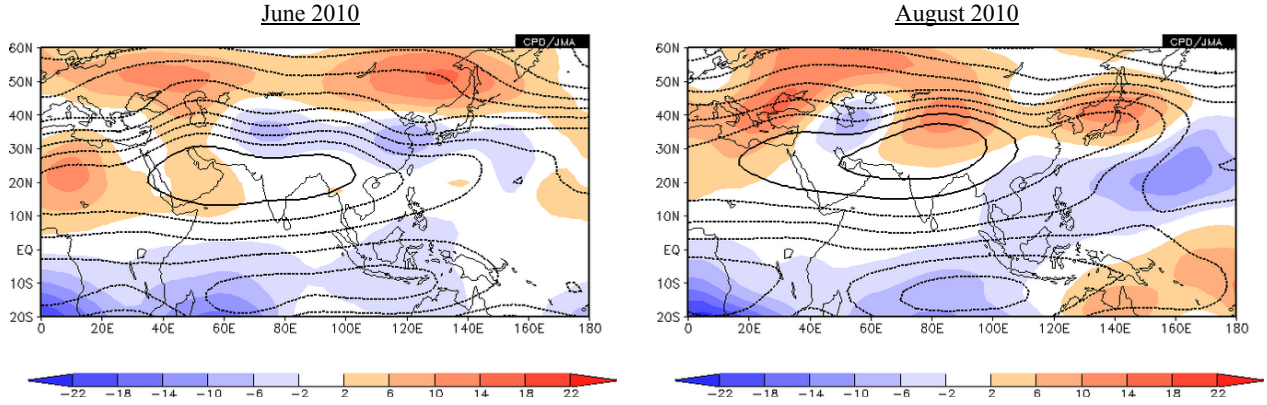

Figure 26 Monthly-mean 200-hPa stream function and anomaly
The contours show the stream function at intervals of 1 x 10^7 m^2/s, and the shading indicates stream function anomalies. In the Northern (Southern) Hemisphere, warm (cold) colored shading denotes anticyclonic (cyclonic) circulation anomalies. The base period for the normal is 1979 – 2004. The analysis data are JRA-25/JCDAS.

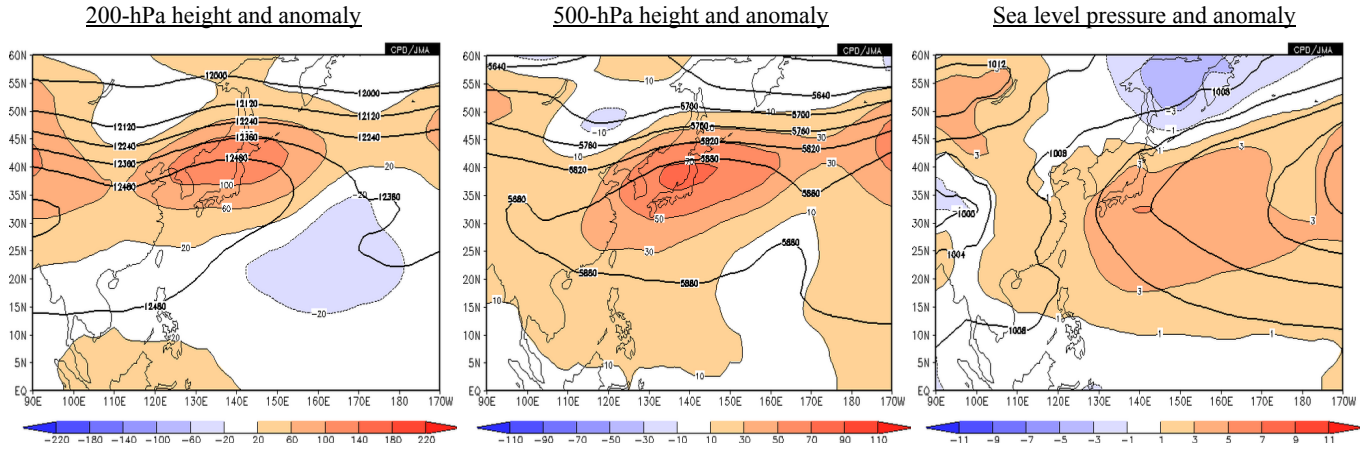

Figure 27 Monthly-mean atmospheric circulation around Japan (August 2010)
Panel on the left: The contours indicate 200-hPa height at intervals of 120 m. Central panel: The contours indicate 500-hPa height at intervals of 60 m. Panel on the right: The contours indicate sea level pressure at intervals of 4-hPa. The shading shows their anomalies. The base period for the normal is 1979 – 2004. The analysis data are JRA-25/JCDAS.

the Asian summer monsoon and the subtropical jet stream in the vicinity of Japan (Figure 28). The results indicated that when convective activity is enhanced (or suppressed) over the region from the northern Indian Ocean to the northeast of the Philippines (10˚N – 20˚N, 60˚E – 140˚E), the subtropical jet stream near Japan tends to shift northward (or southward) from its normal position. Furthermore, a similar statistical examination was implemented in which the region for averaging convective activity was expanded to a wider area in and around the tropical Indian Ocean and the Maritime Continent (10˚S – 20˚N, 60˚E – 140˚E). The results showed that when convective activity is enhanced over this wider area, the subtropical jet stream near Japan tends to shift northward from its normal position (figure not shown).

It therefore seems that the northward shift of the subtropical jet in the vicinity of Japan was associated with active convections over the broad region in and around the Indian Ocean. In addition, considering previous studies (e.g., Nitta, 1987) indicating the influence of convective activity around the Philippines on Japan, active convections from the northern South China Sea to the area to the northeast of the Philippines may have been partly responsible for the strength of anticyclones around Japan, especially from the second half of August to early September.

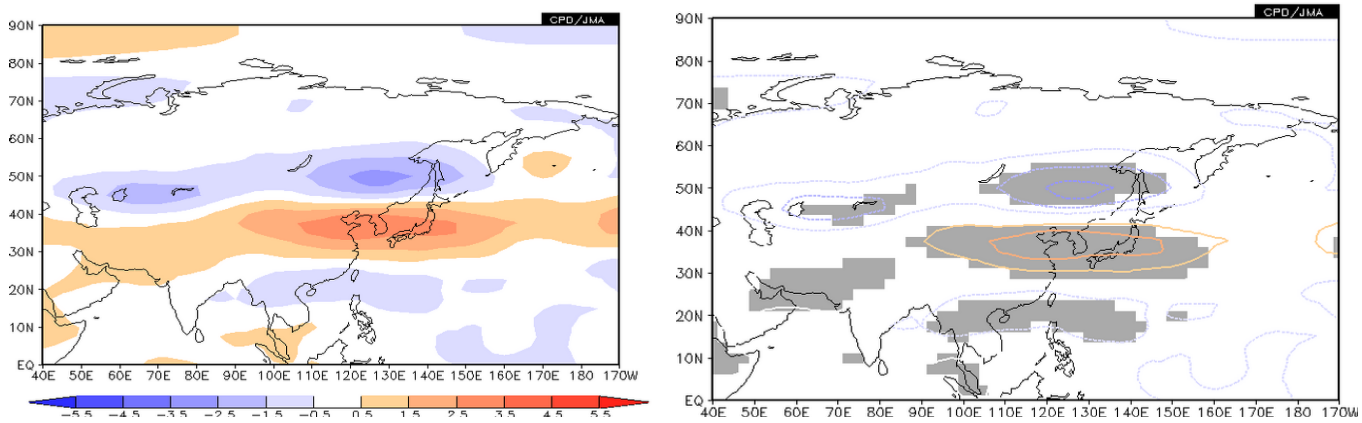

Figure 28 Linear regression coefficients of 200-hPa zonal wind speed onto area-averaged convective activity (OLR) over the region from the northern Indian Ocean to the area to the northeast of the Philippines (10˚N – 20˚N, 60˚E – 140˚E) for July and August
The panel on the left indicates that when convective activity was enhanced (suppressed) over the region, the subtropical jet stream was stronger (weaker) than normal in the cold (warm) colored shading. Panel on the right: the shading shows a 95% confidence level based on F-testing. The base period for the statistical analysis is 1979 – 2009. The analysis data are JRA-25/JCDAS.

(3) Okhotsk High

The Okhotsk High (a cool semi-stationary anticyclone) often develops around the Sea of Okhotsk from spring to autumn and occasionally brings cool air to the Pacific side of northern and eastern Japan, resulting in cool summers. A blocking high in the upper troposphere over the Sea of Okhotsk plays an integral role in the formation of the Okhotsk High (Nakamura and Fukamachi, 2004). In July 2003, in association with the development of an upper-level blocking high over the Sea of Okhotsk, the Okhotsk High appeared and persisted throughout the month, bringing about significantly below-normal temperatures in northern and eastern Japan (the panels on the right of Figure 29).

In June 2010, warm anticyclones frequently covered Japan, particularly its northern parts (the panels on the left of Figure 29). As a result, temperatures were above normal across most of the country. In the period from June to the first half of July, the Okhotsk High was less developed this year than in past years (Figure 30). In the second half of July, the phenomenon temporarily appeared but influenced Japan little due to the northward shift of the subtropical jet near the country and the strong Pacific High to its east (central panels of Figure 29).

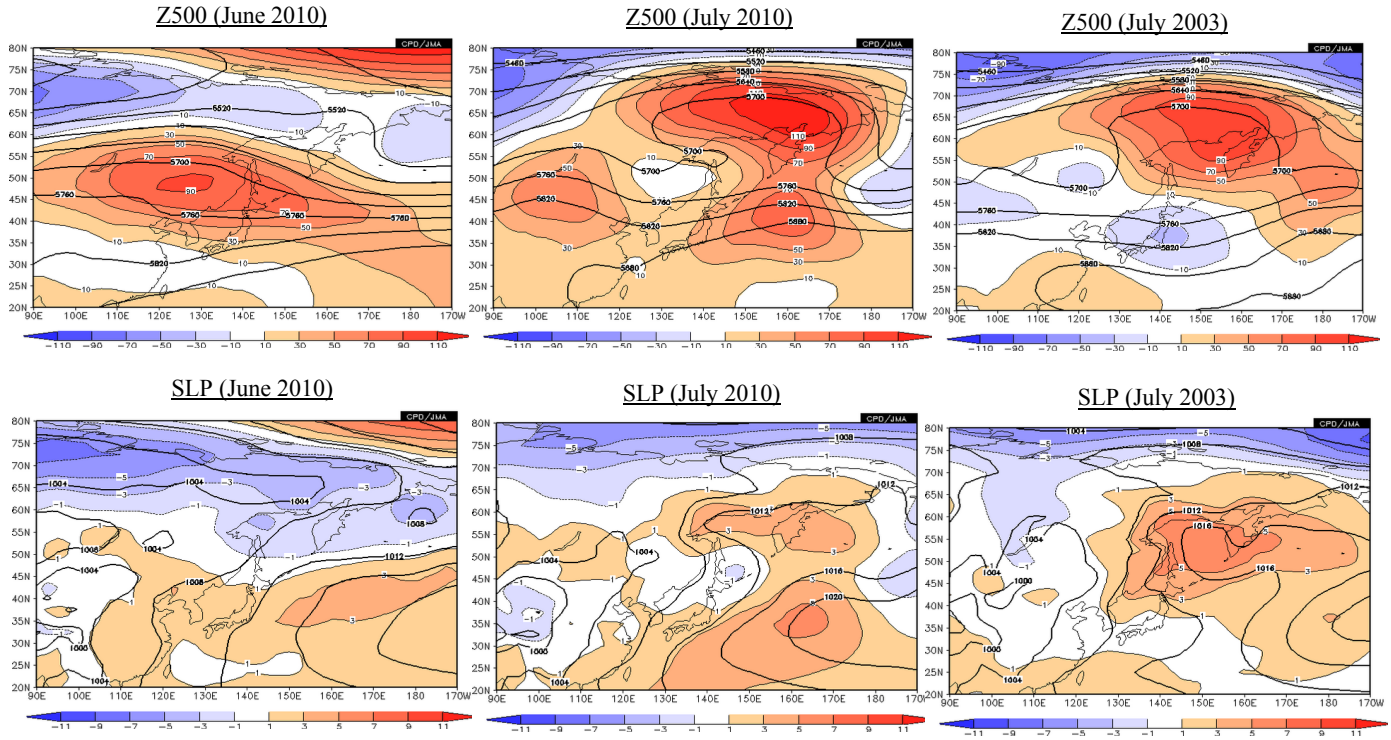

Figure 29 Monthly-mean atmospheric circulation around Japan (left: June 2010; center: July 2010; right: July 2003)
Upper panels: monthly-mean 500-hPa height (thick black contours) at intervals of 60 m and anomaly (shading)
Lower panels: monthly-mean sea level pressure (thick black contours) at intervals of 4 hPa and anomaly (shading)
The base period for the normal is 1979 – 2004. The analysis data are JRA-25/JCDAS.

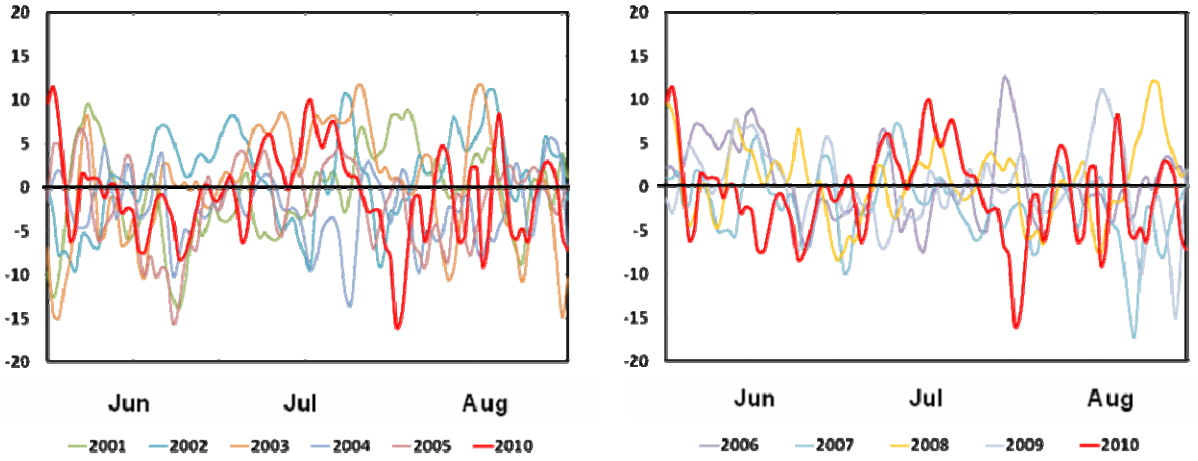

Figure 30 Time series of Okhotsk High Index (2001 – 2010)
The index is the average of sea level pressure anomalies over the Sea of Okhotsk (45˚N – 60˚N, 140˚E – 155˚E). The red lines indicate progression of 2010. The base period for the normal is 1979 – 2004. The analysis data are JRA-25/JCDAS.

4. Conclusion and discussion

The Advisory Panel on Extreme Climate Events identified three atmospheric circulation features related to Japan's extremely hot summer of 2010:

(1) The zonally averaged tropospheric air temperature in the mid-latitudes of the Northern Hemisphere was the highest for June – August since 1979
(2) A remarkably strong anticyclone persisted over Japan
(3) Japan experienced less influence than usual from the Okhotsk High (a cool semi-stationary anticyclone).

These atmospheric features and possible factors contributing to them are illustrated in Figure 31. The above-mentioned primary factors are supported by statistical analysis and research performed to date, but the results of this work do not completely explain the extreme conditions seen. In order to further understand the event and clarify the dynamic mechanism behind it, it is necessary to investigate other possible factors and perform numerical model experiments.

(Shotaro Tanaka, Climate Prediction Division)

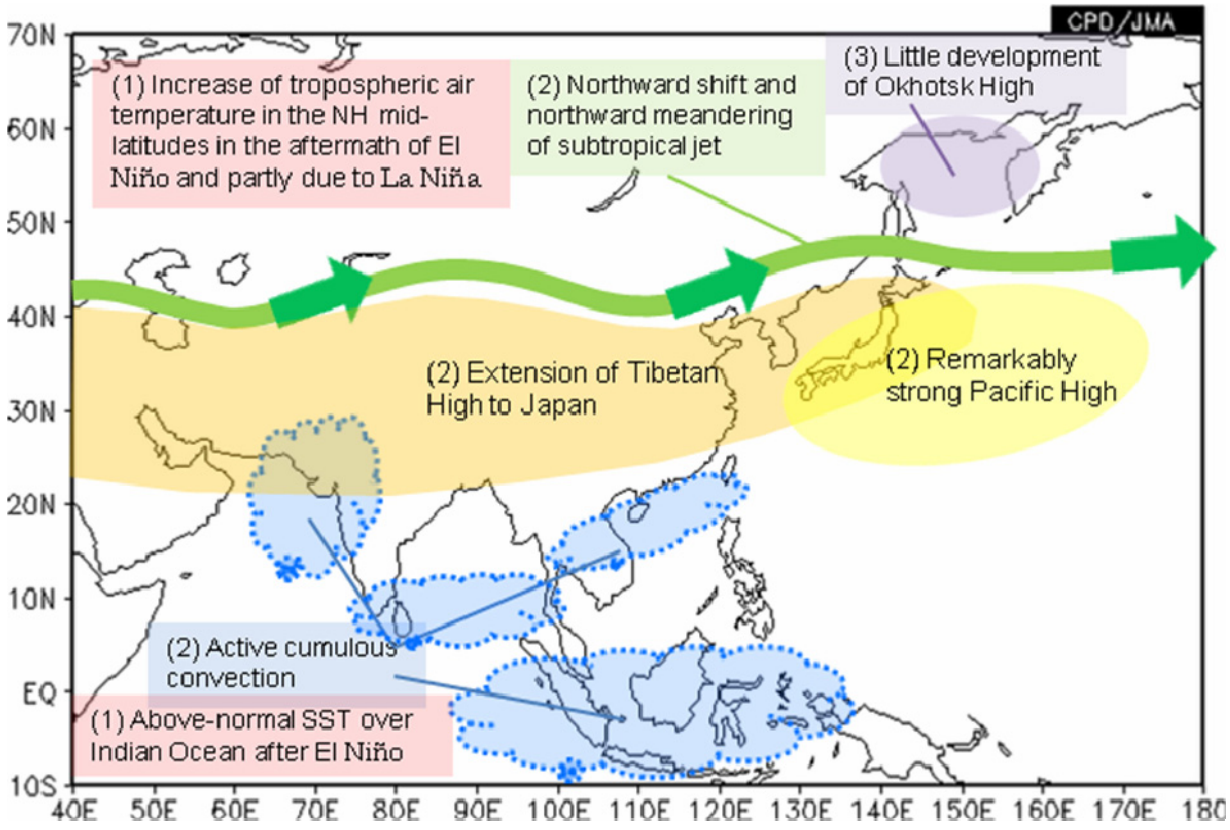

Figure 31 Schematic chart of primary factors contributing to Japan's extremely hot summer (June – August) of 2010
The numbers of (1), (2) and (3) on this chart correspond to those in Section 4 of the main text.

References

Angell, J. K., 1990: Variation in global tropospheric temperature after adjustment for the El Niño influence, 1958-1989, *Geophy. Res. Lett.*, **17**, 1093-1096.

Enomoto, T., 2004: Interannual variability of the Bonin high associated with the propagation of Rossby waves along the Asian jet, *J. Meteor. Soc. Japan*, **82**, 1019-1034.

Krishnan, R. and M. Sugi, 2001: Baiu rainfall variability and associated monsoon teleconnections, *J. Meteor. Soc. Japan*, **79**, 851-860.

Nakamura, H. and T. Fukamachi, 2004: Evolution and dynamics of summertime blocking over the Far East and the associated surface Okhotsk high, *Quart. J. Roy. Meteor. Soc.*, **130**, 1213-1233.

Nitta, T., 1987: Convective activities in the tropical western Pacific and their impact on the Northern Hemisphere summer circulation, *J. Meteor. Soc. Japan*, **65**, 373-390.

Seager, R., N. Harnik, Y. Kushnir, W. Robinson, and J. Miller, 2003: Mechanisms of hemispherically symmetric climate variability, *J. Climate*, **16**, 2960-2978.

Any comments or inquiries on this newsletter and/or the TCC website would be much appreciated. Please e-mail to: tcc@climar.kishou.go.jp
(Chief Editor: Kumi Hayashi)

Tokyo Climate Center (TCC), Climate Prediction Division, JMA
Address: 1-3-4 Otemachi, Chiyoda-ku, Tokyo 100-8122, Japan
TCC website: http://ds.data.jma.go.jp/tcc/tcc/index.html